The effect of the sweep angle to the turbulent flow past an infinite wing

C.A. Suardi, A. Pinelli, and M. Omidyeganeh

1 Introduction

Nowadays the majority of civil aircrafts employs swept-back wings. This configuration, proposed in the early 30's of last century, has been technologically motivated by the otherwise enhanced drag experienced in transonic cruise condition. Since its introduction, several studies have focused on the assessment of the aerodynamic behaviour of this wing configuration for a flow conditions resembling realistic, high Reynolds (Re) number cases of aeronautical interest [1, 2]. In these investigations, the adopted wing model was based on an infinite swept wing with an incoming laminar flow at moderate incidence and at relatively high Re numbers. Under these conditions, the resulting boundary layers undergo an early transition inhibiting the appearence of any major separated regions for a moderate incidence and can thus considered a developing turbulent boundary layer (TBL) subject to a varying adverse pressure gradient (APG). In the present work, we also consider an infinite wing model at a modest angle of attack. However, because of the prohibiting computational cost of detailed simulations at a high Re number, we prefer to mimic this realistic conditions by superimposing free stream turbulence to the approaching clean stream. Indeed, this choice leads to an early by-pass transition that prevent the eventual separation of the TBL, thus leading to a physical situation similar to the reference ones cited above. The high Re number regime, leading to an almost totally turbulent, attached boundary layer, is a quite interesting case for at least two reasons. The first one was put forward long ago and concerns the possibility of predicting the aerodynamic performances of a swept wing (lift and drag) in terms of the associated straight one, using a simple trigonometric function of the introduced sweep angle, suggesting a fairly linear composition of a chordwise and spanwise flow. This property, that has been verified experimentally and numerically by several authors, mainly holds for attached flows and is commonly termed as *Simple Sweep*
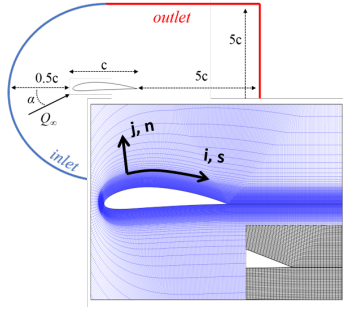
C.A. Suardi · A. Pinelli · M. Omidyeganeh
City, University of London, London, UK, e-mail: carlo.suardi@city.ac.uk

Theory. Although this theory has been the working horse of swept wing design for decades, its exact applicability limits and its extention to other aerodynamic properties is still object of recent investigations. The second aspect that makes the TBL on a swept wing an appealing research topic is related with the comprehension of the structure of the turbulent, wall bounded flow simultaneously exposed to an APG and to an imposed cross flow. An understanding on how these concomitant effects manipulate the structure of the TBL is the central topic of the present contribution. The region of primary interest is the one close to the trailing edge of the wing, where the pressure gradient is a strong adverse one and where the impact of the cross flow generated by the sweep angle is more evident. The effect of the cross flow on the turbulent Reynolds stresses budgets and its eventual impact on the wall regenerating cycle is explored using data from a fully resolved numerical simulation. In particular, is accounted the effect of the sweep adoption on the appearence of *reversed flow nuclei*, similar to those reported into the literature for the high Reynolds TBL subject to zero pressure gradient (ZPG) [3] and for the moderate Re under an APG [7]. In general, our simulations on a straight wing, confirm the appearance of localised and unsteady local separated cores even for the case of an apparently fully attached boundary layer, due to the intense pressure gradient in the latter stage of the wing suction side for the aerofoil and incidence considered. When the 30° sweep-back angle is considered, we observe a mitigation of these reversed flow nuclei, alongside with a not trivial bending of the principal flow structures partecipating in the wall turbulence cycle. Due to the idea put forward by several authors suggesting an eventual link between the mentioned flow structures and the appearence of trailing edge flow separation on a wing, it is believed of great importance to understand how the sweep angle would affect this link. This in order to provide essential guidelines for the development of flow separation devices for the widely adopted swept wings.
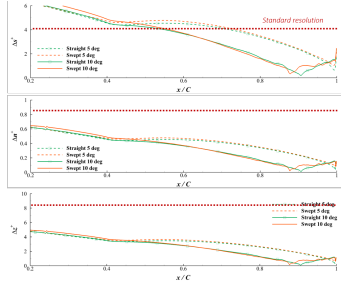
2 Problem Formulation

The flow past an infinite swept wing is dealt with the 3D incompressible, Large Eddy Simulation equations (LES). The region close to the wing surface is fully resolved while the subgrid scale closure is achieved via the ILSA model proposed by Piomelli et al. [4]. This model is based on an adaptive method that triggers the small scales filtering according to a pre-established value of the integral length scale of the turbulent flow. This adaptive feature allows to move from a LES to a pure DNS when approaching the walls or within regions of laminarity and where turbulence decays. The LES equations are space discretised with a second order finite volume method with a co-located formulation on a structured mesh. The use of FFTs allows to take advantage of the assumed periodicity along the spanwise (i.e. *z*) direction, especially when dealing with the pressure Poisson equation arising from the fractional step approach used to advance the equations in time. The solver overall accuracy is second order in both space and time and the MPI library is used in the framework of a domain decomposition approach to exploit parallel, memory dis-

tributed computer architectures. The solver that incorporate all the aforementioned features (called *SUSA*) has been extensively validated in the past [5].The computational domain around each 2D aerofoil (NACA 4412) $x-y$ cross section is sketched in figure 1 alongside with tha wall resolution in inner units (being the friction velocity, u_τ, and the kinematic viscosity, ν). On the $x-y$ plane, the domain is meshed using a body fitted C-grid which 3D extension is achieved extruding the 2D mesh in z using a uniform spacing. A zero velocity boundary condition is enforced at the solid walls, while on the outer boundary (i.e., the surface obtained when extruding the outer 2D boundary in z), we set an inlet/outlet condition that depends on the local, instantaneous direction of the computed flow (Dirichlet condition obtained from an irrotational solution if flow is incoming, non-reflective condition if outgoing) for the x and y velocity components. The swept/unswept wing configuration
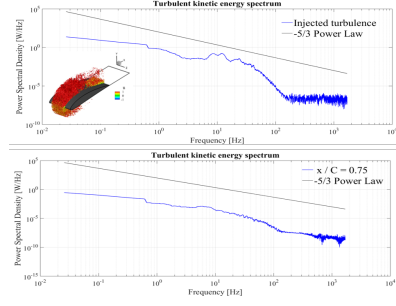

Fig. 1 Domain geometry for the computational study. z extension is $0.4\,c$ (c being the chord size). The domain is assumed to be periodic in z
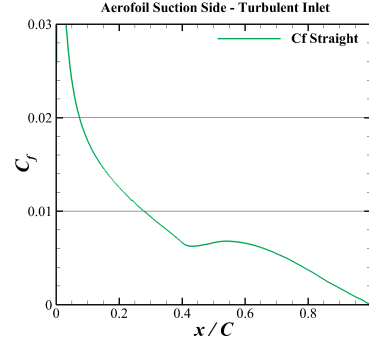

Fig. 2 Wall resolution in plus units for all the cases considered in this investigation, compared with the standard for a turbulent channel flow.

is simulated by setting a constant value for the z velocity component (parallel to the leading edge) on the outer boundary equal to $U_\infty tan(\beta)$, with the sweep angle β, equal to $30^o/0^o$ (U_∞ being the free-stream velocity component perpendiculat to the aerofoil LE). For both swept and unswept cases the chord Reynolds number is $Re_c = U_\infty\,c/\nu = 50 \times 10^3$, and two loading conditions have been considered setting the angle of attack to $\alpha = 5^o/10^o$. The boundary layer transition is triggered by superimposing to the incoming flow a turbulence field (10% intensity) obtained through a twin, independent DNS of grid generated turbulence. In figure 3a is presented the turbulent kinetic energy spectrum of the perturbation introduced, as well as that of the resultant boundary layer in the buffer layer, ($y^+ \approx 25$), at a specific different suction side wing locations, $x/C \approx 0.75$ for the case of un-swept wing at 5° incidence. Inside the in-box it can be found an illustrative sketch of a portion of the grid turbulence introduced into the domain. The effect of the perturbation introduced is that of triggering the boundary layer transition to turbulence via a bypass mechanism from the early stage of the wing. The energized boundary layer does not present a major separation from the wall for the considered incidences,

condition otherwise faced in the absent of boundary layer perturbation [6]. Instead, it remains attached, by statistical mean, until the trailing edge. The coefficient of friction, shown in figure 3b for the case of un-swept wing and 5° incidence, clearly support this statement.

Fig. 3a Turbulent kinetic energy spectrum for the introduced perturbetion (Top) and into the buffer layer for late location on the wing suction side (Bottom). An illustration of the introduced grid turbulence and its effect on the boundary layer is presented into the the squared box.
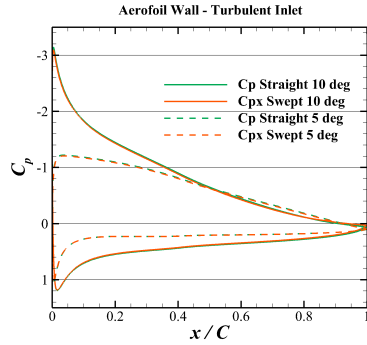

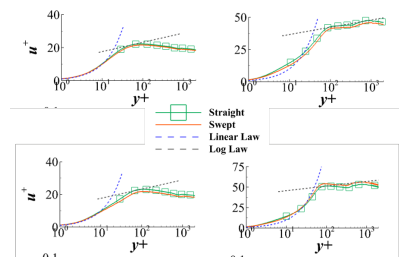**Fig. 3b** Suction side wall friction coefficient along the chord.

3 Results

A comparative study for the effect of a 30° sweep-back adoption on the flow field is made for the two different loading condition considered. Figure 4a presents the mean wall coefficient of pressure, whereas figure 4b presents some chord-wise velocity profile for two consequent chord-wise locations, $x/C = 0.4, 0.95$. The velocity profiles have been scaled with the inner units to make a comparison with the law of the wall in the case of a turbulent channel flow. A good match for both the incidences is found regardless the sweep angle adopted, supporting what has been already postulated as the simple sweep theory for the low order statistics of the turbulent attached flow past an infinite wing [1, 2].

Even though some flow statistics has been found mildly affected by the adoption of the sweep angle, the flow dynamics of the turulent boundary layer results deeply modified. It is reported a varying distortion of the wall turbulence streaks moving toward the trailing edge, especially on the suction side. In figure 5 can be found the contours of the instantaneous wall-normal vorticity fluctuation on a surface above the wing suction side within the buffer layer for both the loading conditions, highlighting the streaks. The effect of the intensifying adverse pressure gradient seems to have a increasingly stronger impact as the streaks are thicker and present a more
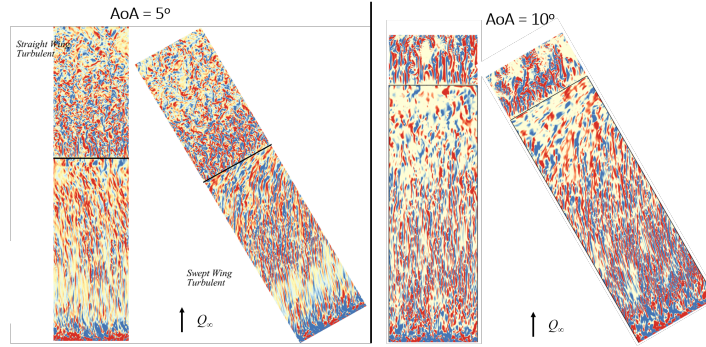
Fig. 4a Distribution of the wall coefficient of pressure for all the cases investigated.

Fig. 4b Profiles of the chord-wise velocity in plus units for the 5° (Top) and 10° (Bottom) incidences, at the chord-wise location $x/C = 0.4$ (Left) and $x/C = 0.95$ (Right), respectively.
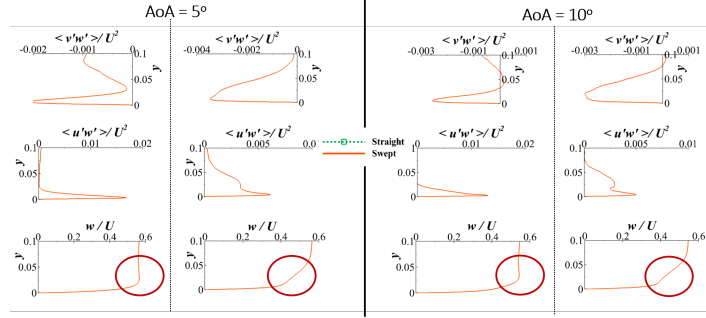
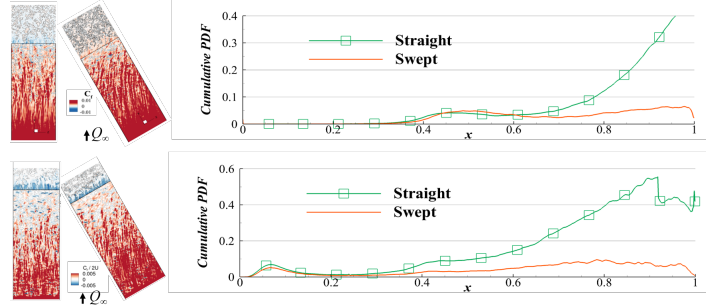meandering pattern. Furthermore, a freshly new turbulent content is detected via the

Fig. 5 Instantaneous iso-contours of the wall-normal component of the vorticity perturbation for the (Left) 5° and (Right) 10° case. The black line identifies the trailing edge. Suction side view.

Reynolds stresses due to the introduced crosswind, for both the incidences, figure 6.

The sweep angle is found to mitigate the reversed flow nuclei appearing inside the wing suction side boundary layer, and thus the portion of the wing interested by reversed flow. Figure 7 presents a map of the instantaneous skin friction on the suction side varying the sweep adopted, alongside with a quantitative account on the same side of the total probability to detect a reversed flow, with respect to the mean flow direction, moving along the chord, for the 5° (Top) and 10° (Bottom) incidence case. What can be qualitatively be observed by the friction map is clearly supported by the mitigated reversed flow region detected on the swept wing, regardless the incidence.

Fig. 6 Time and spanwise averaged profiles of quantities introduced purely by the crosswind for the (Left) 5° and (Right) 10° incidence case. Per each incidence are shown the profiles of the crosswind (Bottom), and two Reynold stresses (Centre and Top), extracted on the suction side at two consequent chord-wise locations, $x/C \approx 0.4$ (Left) and at $x/C \approx 0.95$ (Right).

Fig. 7 (Left) Instantaneous iso-contours of the wall friction and (Right) total probability to detect a reversed flow along the chord for the suction side wall. The (Top) set refer to the 5° incidence case, the (Bottom) one for the 10° case.

References

1. J.M. Altman and N.L.F. Hayter. : A comparison of the Turbulent Boundary-Layer Growth on an Unswept and swept Wing. NACA Technical Note 2500 (1951)
2. Boltz, F. W. and Kenyon, G. C. and Allen, C. Q. : Effects of sweep angle on the boundary-layer stability characteristics of an untapered wing at low speeds. NASA D-338 (1960)
3. Brücker C.: Evidence of rare backflow and skin-friction critical points in near-wall turbulence using micropillar imaging. Phys Fluids. **27**, 031705 (2015)
4. Piomelli, U. and Rouhi, A. and Geurts, B. J.: A grid-independent length scale for large-eddy simulations. J.F.M. **766**, 499–527 (2015)

5. Rosti, M.: Direct numerical simulation of an aerofoil at high angle of attack and its control. City, University of London, London (2016)
6. C.A. Suardi and A. Pinelli and M. Omidyeganeh: Investigation of the Sweep Independence Principle for transitional regime of the flow past an aerofoil. EPSRC UK Turbulence Consortium Meeting, London (2018)
7. R. Vinuesa and R. Örlü and P. Schlatter: Characterisation of backflow events over a wing section. Jour. of Turb. **18.2**, 170–185 (2017)